Evolvability of the Primate Pelvic Girdle

Kristi L. Lewton

Abstract The ilium and ischiopubic bones of the pelvis arise from different regulatory pathways, and as a result, they may be modular in their organization such that features on one bone may be morphologically integrated with each other, but not with features on the other pelvic bone. Modularity at this gross level of organization can act to increase the ability of these structures to respond to selection pressures (i.e., their evolvability). Furthermore, recent work has suggested that the evolution of the human pelvis was facilitated by low levels of integration and high levels of evolvability relative to other African apes. However, the extent of morphological integration and modularity of the bones of the pelvic girdle is not well understood, especially across the entire order of primates. Therefore, the hypothesis that the ilium and ischiopubis constitute separate modules was tested using three-dimensional landmark data that were collected from 752 pelves from 35 primate species. In addition, the hypothesis that the human pelvis demonstrates greatest evolvability was tested by comparing it to all other primates. The results demonstrate that regardless of phylogeny and locomotor function, the primate pelvis as a whole is characterized by low levels of overall integration and high levels of evolvability. In addition, the results support the developmental hypothesis of separate ilium and ischiopubis modular units. Finally, all primates, including humans, apparently share a common pattern of integration, modularity, and evolvability in the pelvis.

Keywords Integration · Modularity · Adaptation · Bipedality · Hominin · Pelvis

Introduction

Pelvic morphology is largely shaped by selection on locomotor and obstetrical functions, but efforts to attribute specific aspects of pelvic shape to particular functional demands have met only limited success. Previous work on human and non-human primates has examined individual aspects of pelvic structure, identified particular traits that are purported adaptations for locomotion, and inferred locomotion in fossil species (e.g., Robinson 1972; Lovejoy 1975; Ashton et al. 1981; Stern and Susman 1983; Fleagle and Anapol 1992; Anemone 1993; MacLatchy 1998; Bramble and Lieberman 2004; Lovejoy et al. 2009; Berger et al. 2010). However, understanding primate pelvic adaptation in response to selection pressures requires not only an understanding of the functional relevance of pelvic structure, but also information on patterns of morphological integration, constraint, and evolvability.

Patterns of integration and parcellation contribute to evolvability—the ability to respond to selection (Hansen and Houle 2004, 2008)—through the relaxation of constraints and the ability to compartmentalize functions and the structures that produce them. Patterns of correlation and covariation of phenotypic traits (i.e., morphological integration sensu Olson and Miller 1958) are caused by selection on traits that share a biological function, by evolutionary conservation of developmental regulatory genes, and by genes with pleiotropic effects on several

K. L. Lewton (✉)
Department of Human Evolutionary Biology, Harvard University, 11 Divinity Ave, Cambridge, MA 02138, USA
e-mail: klewton@fas.harvard.edu

structures. Integrated traits then evolve together, resulting in genetic integration via pleiotropy, and consequently in developmental and evolutionary integration (e.g., Cheverud 1982; Cheverud et al. 1989; Wagner 1996; Hallgrímsson et al. 2009). Morphologically integrated suites of characters can be modular, such that sets of characters are relatively uncorrelated with other sets of characters (e.g., Wagner 1996; Klingenberg 2008; Mitteroecker and Bookstein 2008; Hallgrímsson et al. 2009). Both morphological integration and modularity are therefore identified through the examination of patterns of genetic covariance. However, relevant quantitative genetic data are often missing. Cheverud (1988) compared patterns of phenotypic and genetic covariances and found that under certain conditions (e.g., with large samples of heritable morphological traits), genetic and phenotypic correlation-covariance patterns are broadly similar. While many subsequent researchers have assumed agreement between phenotypic and genetic patterns of covariance for traits of interest, similarity has not been demonstrated for the full range of morphological data, and some caution against the substitution of phenotypic for genetic covariances (e.g., Willis et al. 1991).

Previous work on skeletal integration and modularity in primates has focused on patterns of integration in the skull (e.g., Cheverud 1982, 1995, 1996b; Ackermann and Cheverud 2000; Strait 2001; Marroig and Cheverud 2004a, b; Hallgrímsson and Lieberman 2008; Bastir and Rosas 2009) and limb (Young 2006; Rolian 2009; Williams 2010; Villmoare et al. 2011). While there is a dearth of research on genetic and phenotypic integration of pelvic traits (but see Carrier et al. 2005; Grabowski et al. 2011), there has been some progress in studies of embryology and genetic regulation of pelvic development in birds, amphibians, fish, and mice.

The adult pelvic girdle comprises three bones (the ilium, ischium, and pubis) that arise from separate chondrification and ossification centers to fuse at the acetabulum (Adair 1918). The pelvic girdle develops from a single mesenchymal condensation of lateral plate mesoderm (Chevallier 1977; Malashichev et al. 2008; Pomikal and Streicher 2010). The cartilaginous condensations of what will later be the ilium, ischium, and pubis arise from this common mesenchyme between 34 and 36 days in human embryos (Laurenson 1964; O'Rahilly and Gardner 1975). The ilium begins formation first, followed by the joint formation of the ischium and pubis (Malashichev et al. 2005).

There is a distinct difference in the genetic regulation and morphogenetic interactions of the proximal and distal aspects of the pelvic girdle. Normal development of the ilium requires signaling of *Emx2*, a homeobox-containing transcription factor, from the paraxial mesoderm (whereas the ischium and pubis develop normally without it,

Pellegrini et al. 2001; Malashichev et al. 2008). The ilium does not interact with the vertebral column until the final stages of embryonic development (Theiler stages 24+ to 25+ in the mouse, Pomikal and Streicher 2010; Pomikal et al. 2011), which suggests that ilium formation is not determined by growth of the vertebral column.

The ischium and pubis, on the other hand, both require *Pax1*, a paired-box containing gene, and *Alx4*, a homeobox-containing transcription factor, for normal development (Malashichev et al. 2008). In addition to these genetic inputs, the ischium and pubis interact closely with the femur throughout the entirety of development (Pomikal and Streicher 2010), and when it is not present (e.g., in limb ablation experiments), the ischiopubis does not develop normally (Malashichev et al. 2005).

The formation of the ilium and ischiopubis through different developmental pathways suggests that patterns of pelvic integration and modularity may also be organized according to differences in developmental genetics. Specifically, pelvic anatomy may be developmentally, and consequently evolutionarily, integrated (sensu Cheverud 1996a) according to the genetic regulation of its bony units, such that traits on the ilium are primarily correlated with each other, while those on the ischiopubis are similarly correlated (see, e.g., Atchley and Hall 1991; Zelditch et al. 2009). Strong internal integration of the ilium and ischiopubis would suggest that these structures may be developmental modules, but this is not necessarily a given. For example, the features of the ilium and ischiopubis could be both internally correlated as well as correlated across these two pelvic regions (such that all traits on both structures are correlated with each other). Therefore, a secondary hypothesis is that the ilium and ischiopubis may comprise developmental modules in which features within each structure are highly integrated, but there is no correlation between the two structures.

This study tests the developmental hypothesis that the primate ilium and ischiopubis are separate modules (at this gross level of organization, a pelvic module is defined as a set of morphologically integrated pelvic traits that are uncorrelated with other sets of integrated pelvic traits). That is, ilium traits will be correlated with each other, ischiopubic traits will be correlated with each other, but traits on the ilium will not be correlated with those on the ischiopubis. Additionally, preliminary tests are performed to examine the modularity of the ischium and pubis separately; due to the shared developmental genetic regulation of the ischium and pubis, the prediction is that they are not separate modules. Because understanding patterns of integration, constraint, and evolvability of human pelves requires that they are placed within a broader, comparative context, additional hypotheses regarding the similarity of the pelvis of *Homo sapiens* to other apes, and to primates in

general, will be tested. It has been suggested that the evolution of the human pelvis through selection for bipedality was facilitated by decreased levels of integration and increased evolvability relative to other hominoids (Grabowski et al. 2011). This study tests Grabowski et al.'s (2011) hypothesis that the human pelvis is characterized by the lowest levels of integration and highest levels of evolvability compared to other hominoids, and examines this comparison within a comparative primate framework. If *H. sapiens* is found to have levels of integration and evolvability on par with other primates, then this explanation of how the human pelvis evolved must be reconsidered.

Methods

Three-Dimensional Landmarks and Samples

To examine the extent of morphological integration and modularity in the primate pelvis, three-dimensional (3D) landmark data were collected on 752 bony pelves of 35 primate taxa using a Microscribe G2X point digitizer (Table 1; Fig. 1). Unlike the cranium, there are few Type I landmarks on the pelvis (sensu Bookstein 1991); as a result, most landmarks collected here are Type II, but some Type III landmarks were also used (Fig. 1; Table 2). Landmarks were generally collected on the right side of the pelvis, but when it was not available, landmarks on the left side were collected and the antimeres used.

Landmark data were collected twice for most specimens. Measurement error was calculated using a subsample of taxa chosen to reflect a range of body sizes and taxonomic groups (*Gorilla*, *Saimiri*, *Homo*, *Nasalis*, and *Lepilemur*) following McNulty (2005). Five individuals from each species were analyzed to derive mean measurement errors across both species and landmarks. For each individual, two complete landmark configurations were collected. Mean values were calculated for each landmark (i.e., the mean of the two replicates) and the deviations from individual landmark replicates to the mean landmark were recorded as Euclidean distance. The mean deviation of the two replicate landmark deviations was then calculated and scaled by the Euclidean distance between the landmark mean to the specimen centroid and multiplied by 100 to derive a percent error. The values for each individual were averaged within species, and the interspecific mean landmark deviations and coefficients of variation were calculated (Table S1). Across species, the mean landmark error is 0.32 mm (range: 0.21–0.48 mm) and mean percent error is 1.62% (range: 0.64–2.86%); levels of landmark errors show no relationship to landmark type (i.e., Type II versus Type III landmarks, Figure S2).

Because primates are diverse in their ecological and locomotor specializations—and thus their limb morphologies—a broad sample of primates was measured, including data from strepsirrhines, which are often excluded from analyses of primate morphology. In all species, an effort was made to sample equal numbers of males and females. In addition, some taxa have small sample sizes due to the rarity of complete adult postcranial elements in museum collections. Only adult specimens were used; classification of adulthood was based on sufficient epiphyseal fusion of the iliac crest and ischial tuberosity to permit collection of all anatomical landmarks.

Data Analysis

To assess overall levels of morphological integration in the pelvis, 12 univariate measures were created from the 3D landmarks (Table 3). Linear measures were calculated using interlandmark Euclidean distances, while cross-sectional areas were estimated either by the area of a triangle formed by three 3D landmarks (in the ilium), or the area of an ellipse formed by the maximum and minimum skeletal element dimensions derived from caliper measures (on the ischium) (Lewton 2010). The square root of areal measures was used in all analyses.

Analyses of morphological integration are strongly influenced by many sources of variation in the data such that variation due to sexual dimorphism in body size, differences in rearing environment, the presence of outliers, and the effects of small sample sizes can all result in inflated measures of integration. The dataset used here derives from that of Lewton (2010) and only non-outlying individuals were chosen for analysis (defined as those with standardized residuals greater than ±3). Species-specific samples were examined first for sex-specific rearing differences between wild and captive-bred individuals, and then for intraspecific sex differences. For each set of comparisons, analyses of variance were used to determine equality of sample means, and when no differences were found, samples were pooled. When differences were found, the means of the groups were adjusted such that the difference in means between the two groups was added to the group with the smaller mean. In addition, to ameliorate the effects of small sample sizes, some species were pooled when an ANOVA found no differences in means of raw univariate measures among species, and when the species shared similar ecological variables (e.g., body size, ecological niche, locomotion). Taxon-specific sample sizes ranged from 2 to 45, and when mean-adjusted and pooled, from 10 to 45. A list of all species that are subsumed within pooled taxa may be obtained from the author.

To account for the allometric effects of body size variation on univariate pelvic measures, all individuals within a taxon were first adjusted using the coefficient of allometry,

Table 1 Taxon list and mean measures of integration and evolvability

Taxon	♀	♂	Unknown	Total N	VE	r	r^2	f
Cercopithecoids				218	0.18	0.34	0.16	0.72
Cercopithecus mitis	13	10	1	24	0.07	0.20	0.07	0.50
Chlorocebus aethiops	9	10	1	20	0.14	0.30	0.13	0.72
Miopithecus talapoin	11	4		15	0.22	0.40	0.20	0.61
Cercocebus torquatus	5	5	1	11	0.19	0.35	0.18	0.80
Papio hamadryas	14	23	8	45	0.21	0.39	0.19	0.88
Macaca nemestrina	3	9	1	13	0.43	0.60	0.39	0.82
Macaca fascicularis	13	21	3	37	0.13	0.30	0.12	0.73
Colobus guereza	12	7	4	23	0.07	0.21	0.07	0.72
Procolobus badius	5	5		10	0.18	0.34	0.17	0.67
Nasalis larvatus	7	11	2	20	0.12	0.28	0.11	0.76
Hominoids				168	0.10	0.25	0.09	0.73
Hylobates hoolock	6	7		13	0.11	0.26	0.10	0.71
Hylobates lar	11	13		24	0.08	0.23	0.07	0.69
Symphalangus syndactylus	8	2		10	0.15	0.31	0.14	0.45
Gorilla gorilla	10	11		21	0.08	0.22	0.07	0.73
Homo sapiens	20	20		40	0.10	0.25	0.09	0.82
Pan troglodytes	21	20		41	0.05	0.18	0.05	0.90
Pongo pygmaeus	2	15	2	19	0.16	0.32	0.14	0.84
Platyrrhines				139	0.17	0.33	0.16	0.67
Alouatta caraya	10	10		20	0.16	0.33	0.15	0.71
Ateles spp.	9	11	1	21	0.11	0.26	0.10	0.65
Lagothrix lagotricha	3	6	1	10	0.29	0.44	0.27	0.81
Cebuella pygmaea	5	7		12	0.21	0.37	0.19	0.51
Leontopithecus spp.	10	9		19	0.10	0.25	0.09	0.63
Cebus albifrons	8	7		15	0.24	0.42	0.22	0.80
Cebus apella	8	14		22	0.10	0.26	0.09	0.68
Saimiri spp.	10	10		20	0.15	0.32	0.13	0.56
Strepsirrhines				227	0.15	0.31	0.14	0.65
Lepilemur spp.	12	8		20	0.36	0.54	0.33	0.80
Propithecus spp.	6	9	19	34	0.10	0.24	0.09	0.68
Eulemur fulvus	12	4	6	22	0.06	0.19	0.06	0.48
Hapalemur spp.	6	3	7	16	0.12	0.27	0.11	0.58
Lemur catta	3	6	14	23	0.12	0.27	0.11	0.64
Varecia variegata	2	5	7	14	0.22	0.38	0.20	0.74
Perodicticus potto	3	11	10	24	0.16	0.32	0.14	0.72
Nycticebus coucang	4	4	7	15	0.16	0.32	0.14	0.67
Galago senegalensis	10	15	5	30	0.10	0.26	0.09	0.59
Otolemur crassicaudatus	6	23		29	0.11	0.28	0.10	0.60
Minimum				10	0.05	0.18	0.05	0.45
Maximum				45	0.43	0.60	0.39	0.90
Mean				21	0.15	0.31	0.14	0.69

VE standardized variance of eigenvalues, *r* mean Pearson correlation, r^2 mean squared Pearson correlation, *f* evolutionary flexibility, mean cosine of the angle between selection and response vectors (i.e., vector correlation)

and then by the average group size. Because body mass data are unavailable for many of the individuals examined here, a geometric mean (GM) of the 12 univariate measures was taken as an overall measure of size. For each taxon, the average GM was calculated and logged, and each logged univariate measure was regressed on the average GM. Following Marroig and Cheverud (2004a) and Rolian (2009), the slopes of each regression were used to adjust
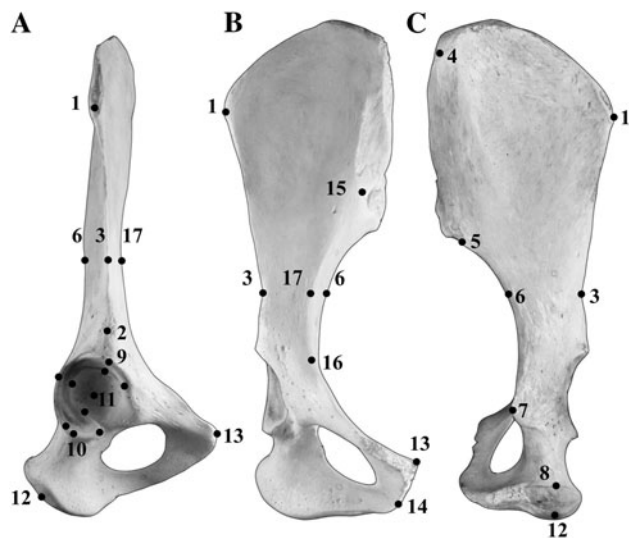
Fig. 1 Three-dimensional landmarks in lateral (**a**), ventral (**b**), and dorsal (**c**) views

the data for each individual using Lleonart et al.'s (2000) method:

$$Y_i^* = Y_i \left(\frac{X_0}{X_i} \right)^b$$

where Y_i^* is the theoretical value of a trait given the taxon average size for individual i, Y_i is the value of the trait for individual i, X_0 is the taxon average size (average GM), X_i is the overall size for individual i (GM), and b is the coefficient of allometry for the regression of the logged trait on log GM. Subsequent to Lleonart et al.'s (2000) procedure, allometrically adjusted data for each individual were then adjusted by its average taxon size.

Integration

Overall levels of integration were examined using average Pearson product-moment trait correlations, average

Table 2 Three-dimensional landmarks

No.	Landmark	Definition	Type
1	ASIS	The anterior-most point on the lateral extent of the iliac crest (anterior superior iliac spine); site of attachment for *m. sartorius*	II
2	AIIS	The anterior-most point on the anterior inferior iliac spine. If only a bony roughening, the point in the center of the AIIS rugosity; site of attachment for *m. rectus femoris*	II
3	Lateral ilium	The lateral-most point on the lateral aspect of the iliac margin, above the AIIS, where the cross-section of the lower ilium is smallest	III
4	PSIS	The superomedial-most point on the posterior iliac crest	II
5	Inferior auricular surface	The inferior-most extent of the auricular surface, on the dorsal aspect of the pelvis	II
6	Dorsal ilium	The dorsal-most point on the dorsal aspect of the lower ilium, where the cross-section of the lower ilium is smallest. Taken directly across from Landmark 3	III
7	Ischial spine	The dorsal-most projection of the spine located on the posterior ischium, medial to the acetabulum	II
8	Ischial tuberosity	The dorsal-most point on the posterior ischium, medial to the acetabulum	II
9	Superior acetabulum	The point on the superior rim of the acetabulum that marks the intersection of the iliac margin and acetabulum, which is defined as the extension of the line connecting ASIS and AIIS	III
10	Inferior acetabulum	The point on the inferior rim of the acetabulum directly across from Landmark 9, along the long axis of the ischium	III
11	Mid-acetabulum	The center of the acetabulum; defined as the midpoint of the line between Landmarks 9 and 10	III
12	Ischium	The distal-most point on the ischium that forms a line with the center of the acetabulum that is parallel to the long axis of the ischium	III
13	Superior pubic symphysis	The superior-most point on the pubic symphysis, taken on the most medial point of the pubis	II
14	Inferior pubic symphysis	The inferior-most point on the pubic symphysis, taken on the most medial point of the pubis	II
15	Lateral sacrum[a]	The point that marks the intersection of the arcuate line of the ilium and the sacrum	I
16	Transverse diameter of pelvis[a]	The point on the arcuate line that constitutes the maximum distance between the arcuate line of the opposing os coxa	II
17	Medial ilium	The medial-most point on the medial aspect of the lower ilium, where the cross-section of the ilium is the smallest. Taken directly across from Landmarks 3 and 6	III

[a] From Tague (2005)

Table 3 Linear measures derived from interlandmark distances

Linear measure	Interlandmark distance/definition
Superior pubic ramus length	11–13
Inferior pubic ramus length	12–14
Pubic symphysis length	13–14
Ilium length	1–9
Lower iliac height	5–11
Ischium length	11–12
Acetabulum diameter	9–10
Ilium width	1–4
Lower ilium cross-sectional area	Area formed by L3, 6, 17
Ischium cross-sectional area	Ischium width × ischium depth
Pelvis length	Ilium length + ischium length

squared correlations, and eigenvalue variance of the univariate measures. Taxon-specific, pooled within-group trait correlation and covariance matrices were generated using casewise deletion for missing observations. These matrices are the data on which all subsequent analyses were performed. All tests were performed in R (R Development Core Team 2011) unless otherwise noted.

Eigenanalysis was used to quantify integration (e.g., Wagner 1984; Cheverud et al. 1989; Villmoare et al. 2011). When traits are correlated most of the variation resides in the first few dimensions of a principal components analysis, which increases variance of the eigenvalues of the first eigenvector. Eigenvalue variance of the correlation matrix was standardized by the maximum possible eigenvalue variance to allow comparison of eigenvalue variances across taxon-specific matrices that may differ in size (Pavlicev et al. 2009):

$$VE_{SD} = \frac{VE}{N-1}$$

where VE_{SD} is the standardized eigenvalue variance, VE is the observed eigenvalue variance, and N is the number of traits in the correlation matrix ($N-1$ is the maximum eigenvalue variance, Pavlicev et al. 2009). This process was repeated for each taxon-specific trait correlation matrix.

Variance of eigenvalues was compared across species using bootstrap resampling methods (Manly 1997). For each species, the original data matrix was bootstrapped 1,000 times, a correlation matrix was derived from each bootstrap sample, and VE was calculated from each of the 1,000 correlation matrices. Statistical significance of interspecific pairwise comparisons was obtained using a difference of means test (as in Scott 2010). For each of the 1,000 VE replicates of two species, the difference between the two species was calculated. This created a distribution of differences in VE replicates that was then zero-centered.

Each of the zero-centered differences was then compared to the observed difference in VE between the two species. The two-tailed P value was calculated as the number of times the difference from the zero-centered distribution was equal to or greater than the observed difference between the two species' VE, divided by the number of bootstrap replicates (Manly 1997). Pairwise comparisons of VE were calculated for all 35 taxa.

To examine how patterns of trait correlation and covariation in humans relate to hominoids in particular and primates in general, a series of correlations of the taxon-specific correlation matrices were performed using a Mantel test followed by a permutation test for statistical significance (Marroig and Cheverud 2001; Steppan 2004; Goswami 2006a, b). Covariance matrices were compared using the random skewers method (Cheverud 1995; Marroig and Cheverud 2001; Cheverud and Marroig 2007) in which each covariance matrix was subjected to a random selection vector and vector correlations were calculated over 10,000 random selection vectors using Revell's random skewers program (2007). Because estimates of correlation and covariance matrices include error, all matrix correlations were adjusted by the square root of the product of the matrix repeatabilities of each taxon-specific correlation or covariance matrix. For correlation matrices, repeatability was calculated as the difference between the observed and error variance of estimated correlations divided by the observed variance (Cheverud 1996b). Covariance matrix repeatability was calculated using a bootstrap test of self-correlation (Cheverud et al. 1989; Cheverud 1996b) in which the covariance matrix was bootstrapped 1,000 times and each iteration compared to the original sample covariance matrix using the random skewers method (Marroig and Cheverud 2001). The average of these matrix comparisons is the estimate of repeatability (Marroig and Cheverud 2001).

Modularity

Developmental hypotheses of pelvic modularity were tested using Klingenberg's (2009) procedure for 3D landmarks. This method was chosen over approaches using interlandmark measures because of its simplicity and ability to test a priori hypotheses of modularity. Due to the constraints of geometric morphometric analysis, specimens with missing landmarks could not be used, resulting in a slightly different sample of pelves than used in the analyses of integration ($N = 716$ specimens). Landmark coordinates were scaled, translated, and rotated to remove the effects of non-shape parameters using Generalized Procrustes Analysis (Rohlf and Slice 1990; Dryden and Mardia 1998). Procrustes coordinates were regressed on log-centroid size using pooled, within-group covariance, and a permutation

test showed a significant influence of allometry on pelvic morphology ($P < 0.0001$). Therefore, further analyses were performed on the covariance matrix of the residuals of the regression of Procrustes coordinates on log-centroid size (Klingenberg 2009). Landmarks were assigned to the following regions: ilium, ischium, or pubis. Acetabular landmarks were excluded from analyses because developmentally they belong to each of the three pelvic bones. Due to the small number of landmarks located on the ischium and pubis, tests regarding their separate modularity are weak; they are presented here with this caveat. Three specific tests were performed: one that tests for the presence of three modules (ilium, ischium, pubis); one that tests whether the ischium and pubis are separate modules; and one that tests whether the ilium and ischiopubis (i.e., a module that combines both ischium and pubis landmarks) are separate modules. The ilium group comprises nine landmarks, the ischium three, and the pubis two; the combined ischiopubis module has five landmarks.

The statistical test for modularity uses the RV coefficient (Escoufier 1973; Klingenberg 2009), which is similar to a correlation coefficient in that it represents the magnitude of similarity between two matrices (the original name "RV" is derived from the correlation (r) between two vectors (v), Escoufier 1973). The RV coefficient was calculated for the comparison of the proposed modules, and a randomization procedure was then used to permute all possible modules and calculate the RV coefficient for each paired comparison. The RV coefficient calculated for the hypothesized module was compared to the distribution of RV coefficients derived from all possible modules. If the RV coefficient of the proposed module was the smallest, or smaller than most other modules, the test was considered significant (see Klingenberg 2009 for a derivation of this analytical method). All analyses of 3D landmark data were performed in MorphoJ (Klingenberg 2011).

Evolvability

The ability of the pelvis to respond to selection was evaluated using *mean flexibility* (*f*) (Marroig et al. 2009), which is derived from Lande's (1979) multivariate selection equation:

$$\Delta z = G\beta$$

where G is the genetic covariance matrix, β is a selection vector, and Δz is the response vector. Here the phenotypic covariance matrix P is substituted for G because they have been shown to be similarly structured (e.g., Cheverud 1996a; Porto et al. 2009). The covariance matrix for each taxon was subjected to 1,000 randomly generated selection vectors and the angle between the selection and response vectors was calculated for each iteration. The mean cosine of the 1,000 angles between response and selection vectors

(i.e., the vector correlation) is the mean flexibility of the taxon (Marroig et al. 2009), which describes the degree to which the response and selection vectors are aligned in multivariate space. Response and selection vectors that are parallel (i.e., when cosine of the angle between them is 1) indicates a structure that is more responsive to selection, i.e., more evolvable. A larger angle between the response and selection vectors is indicative of less evolvability. In general, high levels of evolvability measures, such as evolutionary flexibility, tend to be associated with low levels of integration measures (e.g., VE).

Pairwise comparisons of evolutionary flexibility across all taxa were performed as described for VE; the distribution of vector correlations obtained from the covariance matrix and 1,000 random selection vectors for any two species were compared using the difference of means test and accompanied by a two-tailed P value.

To examine the effect of phylogenetic relatedness on patterns of morphological integration and evolvability, average squared Pearson trait correlations, standardized eigenvalue variance, and mean evolutionary flexibility were compared among taxa using Blomberg's K statistic (Blomberg et al. 2003). The K statistic for phylogenetic signal has higher power and lower type I error rates than the alternative, the Mantel test (Harmon and Glor 2010). The K statistic compares the observed variance of phylogenetic independent contrasts for a given trait to the expected variance from a random distribution of contrasts obtained by shuffling tip taxa on a phylogeny. A $K \geq 1$ indicates phylogenetic signal, while $K = 0$ indicates an absence of phylogenetic signal; the P value for the K-statistic is derived from a randomization test. A consensus phylogeny based on GenBank data was derived from the *10kTrees* project (version 3, Arnold et al. 2010). Phylogenetic signal analyses were performed using the 'picante' package in R (Kembel et al. 2010). Preliminary analysis using Blomberg's K statistic showed that phylogenetic signal was not detected in any of the measures of integration and evolvability ($K_r^2 = 0.25$, $P = 0.67$; $K_{VE} = 0.25$, $P = 0.65$; $K_f = 0.32$, $P = 0.18$), indicating that any patterns in measures of correlation and covariance among taxa are not due to phylogenetic relatedness. Therefore, the potential effects of phylogeny on patterns of integration are not considered further.

Similarly, the potential effects of functional differences due to locomotion on patterns of correlation among taxa were examined with a phylogenetic ANOVA using the package 'geiger' in R (Harmon et al. 2008). For each dependent variable (r^2, VE, and f), a separate test was conducted with locomotor behavior as the factor and 1,000 permutations for statistical significance. The effects of differing locomotor classification were examined by running separate tests using different factor levels (e.g., a broad group—quadruped, suspensory, leaper, biped—versus

a narrower group—arboreal quadruped, terrestrial quadruped, arboreal leaper, etc.), and all tests were statistically insignificant with $P \gg 0.05$; consequently, these results are not presented here, and the effects of locomotion on measures of trait correlation are not considered further.

Results

The level for significance of pairwise comparisons across all taxa was set at $\alpha = 0.001$ due to the large number of tests performed (595 pairwise comparisons for 35 taxa). For all other statistical tests, the level for statistical significance is $\alpha = 0.05$.

Integration

Mean Pearson correlations for taxon-specific trait correlation matrices indicate moderate variability among taxa (Fig. 2). In general, hominoids have trait correlations lower than the average for primates, ranging from 0.18 to 0.32 (average r among all primates is 0.31) (Table 1). Correlations in other taxa are variable, but phylogenetic trends are not readily apparent (as suggested by Blomberg's test). Some taxa exhibit somewhat high correlations relative to other taxa; *Macaca nemestrina* ($r = 0.60$) and *Lepilemur* spp. ($r = 0.54$) have the highest trait correlations.

Standardized eigenvalue variance of the correlations among univariate pelvic measures also indicates variable levels of integration among primate taxa, with VE ranging from 0.05 to 0.43, and an average VE among all taxa of 0.15 (Fig. 2; Table 1). While there is a lack of overall phylogenetic patterning, hominoids generally demonstrate low VE (mean VE = 0.1, Fig. 3), but some taxa within this clade are exceptions; *Hylobates hoolock* VE = 0.11, *Symphalangus syndactylus* VE = 0.15, *Pongo pygmaeus* VE = 0.16. Like the results for r, some taxa have relatively large VE values; *Lagothrix lagotricha*, *Lepilemur* spp., and *Macaca nemestrina*, have VEs ranging from 0.29 to 0.43 (Table 4).

Comparison of VE among taxa indicates broad similarity across the primate order (Table S3). Pairwise comparisons of VE among all 35 taxa show only seven of the 595 comparisons indicating statistically significant difference. None of the 34 pairwise tests between human and non-human taxa indicate significant difference in VE.

Comparisons of correlation matrices among hominoids only show moderate similarity, with 10 out of 21 paired comparisons being significantly similar (Table 4). Notably, the comparisons among *Homo* and the other hominoids are all significantly similar except for the comparison with *Pongo* (Table 4). Patterns of covariance among hominoids indicate stronger similarity, with *Homo* significantly similar to all other hominoids (Table 5). The null hypothesis of
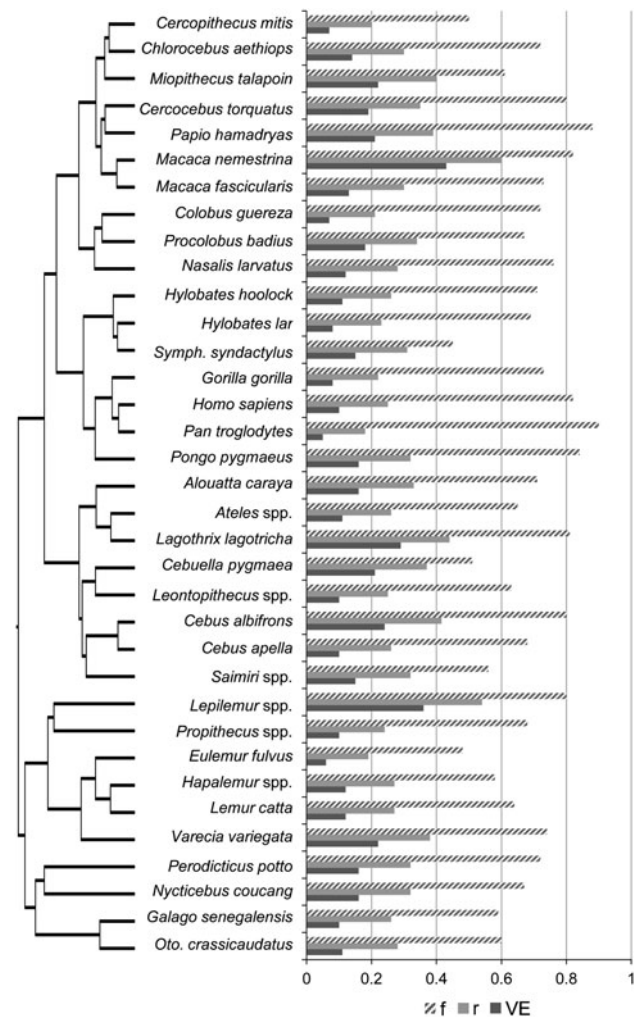
Fig. 2 Phylogeny and bar graph of integration (r and VE) and evolutionary flexibility (f) measures

dissimilarity in covariance structure among taxa is not rejected for the comparisons between *Hylobates hoolock* and *Gorilla* and *Pongo*, as well as between *Pongo* and *Symphalangus*, but these correlations are close to the cut-off value for statistical significance, with P values ranging from 0.05 to 0.06 (Table 5).

Patterns of covariance between *Homo* and all other primate taxa indicate broad similarity (Table 6). Only five out of 34 comparisons are not significant at $P = 0.05$ (these are four cercopithecine taxa and *Saimiri* spp.). If a Bonferroni correction is used to adjust for the number of tests performed, only two tests remain significant at $P < 0.002$ (*Homo* v. *Pan*, $P = 0.0005$; *Homo* v. *Gorilla*, $P = 0.0008$).

Modularity

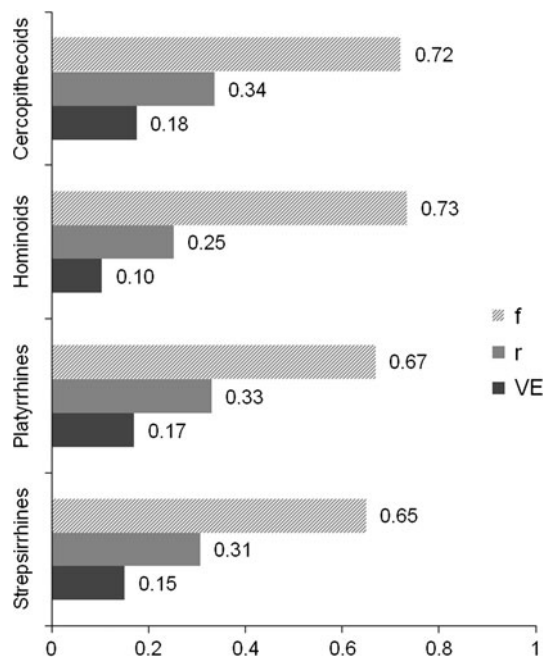The RV coefficient for the proposed ilium and ischiopubis modules is 0.27 and statistically significant ($P < 0.01$),

Fig. 3 Average integration (*r* and VE) and evolutionary flexibility (*f*) measures for the four major primate clades examined here

indicating that the hypothesis of modularity is supported. Of the 2002 possible partitions, only 21 have an RV coefficient less than the proposed module (Fig. 4), and the

partition with the smallest RV coefficient has an RV = 0.24. As mentioned previously there are not sufficient landmarks on the ischium and pubis to test the hypothesis of modularity of each of these regions separately. However, with the caveat that future work must include more landmarks in these regions to further investigate the presence of modules, the two tests of separate ischium and pubic modularity were both statistically insignificant: the test that the ilium, ischium, and pubis are three modules had an RV of 0.28 (*P* = 0.25), while the test that the ischium and pubis are two separate modules had an RV of 0.25 (*P* = 0.10).

Evolvability

The mean cosine of the angle between the selection and response vectors—that is, the evolutionary flexibility of the pelvis (*f*)—ranges from 0.45 to 0.90 (Table 1; Fig. 2). Among all taxa, the average evolutionary flexibility is 0.69. Pairwise comparisons of *f* indicate widespread similarity, with only 12% of the 595 tests reaching statistical significance (Table S4). Only six of the 34 comparisons (18%) of *f* between humans and non-humans are significantly different; humans share the same level of evolutionary flexibility with most primates.

Table 4 Results of Mantel tests between each pair of correlation matrices of hominoid taxa

	Homo	Pan	Gorilla	Pongo	Symphalangus	H. hoolock	H. lar
Homo	0.98	**0.007**	**0.03**	0.42	**0.02**	**0.04**	**0.002**
Pan	0.39	0.98	0.08	0.08	**0.001**	**0.01**	**0.008**
Gorilla	0.27	0.19	0.98	**0.03**	0.09	0.31	0.24
Pongo	0.03	0.22	0.29	0.98	0.27	0.3	0.1
Symphalangus	0.32	0.43	0.19	-0.10	0.98	0.07	0.27
H. hoolock	0.23	0.29	-0.07	0.06	0.19	0.98	**0.009**
H. lar	0.40	0.31	0.09	0.17	0.08	0.31	0.98

Correlations are in the lower triangle and are corrected by matrix repeatabilities for each paired comparison, which lie on the diagonal; *P* values are in the upper triangle, bold indicates significance at alpha = 0.05

Table 5 Results of random skewers vector correlations between each pair of covariance matrices of hominoid taxa

	Homo	Pan	Gorilla	Pongo	Symphalangus	H. hoolock	H. lar
Homo	0.84	0.0005	0.0007	0.003	0.04	0.01	0.008
Pan	0.97	0.82	0.002	0.002	0.006	0.002	0.001
Gorilla	0.93	0.88	0.86	0.001	0.04	0.05*	0.02
Pongo	0.83	0.87	0.88	0.87	0.06*	0.05*	0.01
Symphalangus	0.60	0.78	0.59	0.52	0.90	0.019	0.04
H. hoolock	0.70	0.86	0.56	0.54	0.65	0.92	0.003
H. lar	0.77	0.89	0.69	0.72	0.56	0.81	0.88

Correlations are in the lower triangle and are corrected by matrix repeatabilities for each paired comparison, which lie on the diagonal; *P* values are in the upper triangle, * indicates an insignificant result

Table 6 Covariance matrix repeatabilities, correlations, and *P*-values for the comparison of *Homo sapiens* with all other primates
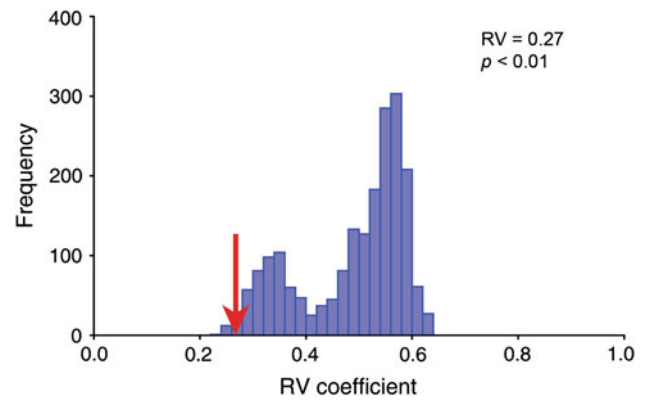
Taxon	*t*	*r*	*P*
Alouatta caraya	0.88	0.73	0.01
Ateles spp.	0.88	0.66	0.02
Cebuella pygmaea	0.88	0.55	0.05
Cebus albifrons	0.88	0.63	0.03
Cebus apella	0.87	0.65	0.02
Cercocebus torquatus	0.90	0.47	0.08*
Cercopithecus mitis	0.88	0.47	0.08*
Chlorocebus aethiops	0.90	0.44	0.09*
Colobus guereza	0.87	0.58	0.04
Eulemur fulvus	0.83	0.73	0.01
Galago senegalensis	0.86	0.81	0.005
Gorilla gorilla	0.85	0.93	**0.0008**
Hapalemur spp.	0.85	0.70	0.02
Hylobates hoolock	0.88	0.70	0.01
Hylobates lar	0.86	0.77	0.007
Lagothrix lagotricha	0.85	0.85	0.004
Lemur catta	0.86	0.78	0.007
Leontopithecus spp.	0.86	0.66	0.03
Lepilemur spp.	0.87	0.80	0.005
Macaca fascicularis	0.87	0.67	0.02
Macaca nemestrina	0.88	0.62	0.03
Miopithecus talapoin	0.89	0.42	0.1*
Nasalis larvatus	0.84	0.70	0.02
Nycticebus coucang	0.87	0.67	0.02
Otolemur crassicaudatus	0.87	0.84	0.004
Pan troglodytes	0.83	0.97	**0.0005**
Papio hamadryas	0.86	0.79	0.006
Perodicticus potto	0.89	0.63	0.03
Pongo pygmaeus	0.85	0.83	0.004
Procolobus badius	0.87	0.71	0.01
Propithecus spp.	0.86	0.74	0.01
Saimiri spp.	0.87	0.55	0.05*
Symphalangus syndactylus	0.87	0.60	0.04
Varecia variegata	0.87	0.74	0.01

t covariance matrix repeatability, *r* correlation coefficient between covariance matrices of *H. sapiens* and each taxon, *P* significance at alpha = 0.5. After Bonferroni, level of significance is 0.001. Bold indicates highly significant tests, * indicates lack of significance at alpha = 0.05

Discussion and Conclusion

Integration

Observed pelvic patterns of correlation and covariation are not obviously related to phylogeny or locomotor function. Overall, the results of integration analyses presented here confirm those of previous studies which have found that hominoids are characterized by low levels of integration—

Fig. 4 Distribution of permuted RV coefficients. *Arrow* denotes RV coefficient for the comparison between hypothesized ilium and ischiopubis modules

as measured by eigenvalue variance, trait correlations, and comparisons of covariance matrices—in both the cranium and postcranium (Young and Hallgrímsson 2005; Marroig et al. 2009; Porto et al. 2009; Rolian 2009; Williams 2010; Young et al. 2010; Grabowski et al. 2011). However, when this result is placed within the larger context of comparative primate patterns of integration, it is not singular: hominoids do have relatively lower levels of integration (i.e., relative trait independence) than other primate taxa, but primates as a clade are generally characterized by low levels of pelvic integration, with only 1% of the interspecific comparisons indicative of significant difference. Indeed, the only significant differences between a hominoid and non-hominoid taxon occurs between *Pan* and *Macaca nemestrina* and *Pan* and *Lepilemur* spp. However, these two taxa (*M. nemestrina* and *Lepilemur*) generally have higher levels of integration than other primates, and are likely driving the two observed pairwise differences. Care was taken to eliminate sex-, size-, and rearing-related sources of variation in trait correlation matrices that might cause erroneous levels of high integration; thus it is unlikely that these results are due to any of these confounds. Another potential cause of these unusually high values is small sample sizes and/or sampling error. Cheverud (1988) has shown that with species samples of fewer than 40 individuals, results of correlation and covariance analyses can be unreliable. However, many of the primate taxa included here have relatively small samples by this standard, but do not deviate substantially from the mean measures of integration.

Modularity

The test of developmental modularity of the pelvis using 3D data strongly supports the hypothesis that the ilium and ischiopubis are modular. The two tests of modularity that

separate the ischium and pubis into individual units were both statistically insignificant, which suggests that the pelvis consists only of two modules: the ilium and the ischiopubis. Together, these results support the predictions that (1) the ilium and ischiopubis are separate developmental modules as a result of their differing genetic regulation pathways and (2) the ischium and pubis comprise one module as a result of their shared genetic and morphogenetic signaling inputs. While these results are suggestive of pelvic modularity as a result of genetic regulation of development, it should be noted that these patterns would also be consistent with other, non-developmental and/or epigenetic causes of phenotypic integration. An additional caveat is that the statistical power required to reject a null hypothesis of lack of modularity is low due to the presence of few landmarks on the ischium and pubis separately. To be confident, therefore, in the developmental hypothesis of pelvic modularity presented here, patterns of modularity must be re-examined with an increased sample of landmarks on the ischium and pubis in conjunction with developmental genetic data on pelvic phenotypes.

The extent of modularity of the ilium and ischiopubis has significant implications for the evolution of the primate pelvis in response to selection for locomotor function. Modules, which are formed when suites of traits undergo parcellation, facilitate evolution by natural selection by permitting change in structural components without necessarily altering other components to the same degree (although some change in other components is inevitable because morphologies are linked at some level of organization) (Riedl 1977; Cheverud 1996a; Wagner 1996; Hallgrímsson et al. 2002; Hallgrímsson et al. 2009; Goswami and Polly 2010). Therefore, if the ilium and ischiopubis are strongly modular, then they may be more "respondable" to selection (sensu Hansen and Houle 2008), which would explain how, for example, the hominin pelvis was able to change so dramatically in a relatively short time period.

To contextualize the relevance of pelvic modularity to the evolution of primate pelves, it is helpful to consider the diversity in ilium morphology that is found among extant primates. Small-bodied vertical clingers and leapers (galagos and tarsiers) and slow-climbing lorises have long, thin rod-like ilia (Jouffroy 1975), while lemurs and indriids have shorter, plate-like ilia. Large-bodied vertical clinging and leaping indriids have particularly unusual ilia that are mediolaterally broad with pronounced anterior iliac spines (both superior and inferior), thought to be related to powerful extension of the thigh during leaping (e.g., Jungers 1976; Sigmon and Farslow 1986). Among haplorhines, ilia are still more blade-like, with the most extreme examples found in the large-bodied African great apes. Compared to all other primates, bipedal hominins may have the most

unusual of ilia: in humans the blade is short and anteriorly curved, relatively robust in thickness of its crest and base (i.e., the lower ilium), and has prominent anterior and posterior spines. Thus, while primates differ in the constraints on and functional requirements of their particular forms of locomotion, they achieve anatomical differences through the same, shared pathways of integration and modularity.

However, it should also be noted that this study considers only a hypothesis of developmental modularity. Additional hypotheses of modularity—perhaps related to adaptive signal of locomotor or obstetrical requirements—also need to be tested. Hypotheses of muscle-bone interactions relevant to locomotor function, for example, could be tested alongside developmental hypotheses of integration (as in Zelditch et al. 2009). For example, one could examine whether patterns of integration of the ilium among primate taxa are related to the insertions of the gluteal, iliopsoas, and hip rotator muscles. Another plausible functional hypothesis is that the obstetrical requirements of large brains relative to body size—a pattern that characterizes primates—may drive patterns of correlation and covariance in primate pelvic shape. This hypothesis could be tested by comparing primates to non-primate mammals, as well as by investigating patterns of pelvic trait covariance in primate taxa that have relatively large brains for body size compared to other primates (i.e., *Saimiri*, *Cebus*, and later fossil hominins and *H. sapiens*). In addition, incorporating data on patterns of covariance in the vertebral column and hindlimb may also help to test both developmental (related to the genetic regulatory mechanisms of pelvic embryology) and functional hypotheses of pelvic integration and modularity.

Primate Evolvability and Adaptation

The ability of the pelvis to respond to selection (evolvability, as measured by evolutionary flexibility) is generally high among primates, both absolutely and in comparison to similar measures for primate limbs and crania (Marroig et al. 2009; Villmoare et al. 2011). Together with the relatively low levels of integration, this result generally confirms those of previous studies that show that primates are characterized by low levels of integration and high levels of evolvability relative to other mammals (Marroig et al. 2009; Porto et al. 2009). More data are necessary to determine how this general primate pattern of pelvic integration and evolvability compares to other mammalian groups.

With respect to the evolution of the human pelvis, these results partially support the argument by Grabowski et al. (2011) that low levels of integration and high levels of evolvability may have facilitated the reorganization of the hominin pelvis coincident with the origins of bipedality.

However, the results presented here for hominoids in general differ somewhat from those presented by Grabowski et al. (2011). In both studies, *Gorilla* has the lowest measures of evolutionary flexibility, but in this study, *Pan* has the highest flexibility measure, while *Homo* does in Grabowski et al. (2011). While the pattern among taxa conflicts in the two studies (although this may be related to sampling differences), the overall pattern is the same: levels of pelvic integration are low and levels of evolutionary flexibility are high. Additionally, the results presented here indicate that there are no significant differences among any of the hominoids in levels of integration, and while there are some differences among hominoids in evolvability, *Homo* is not significantly different from any of the other hominoids. Furthermore, if the hominoid clade is placed within the context of the entire primate order, the pattern of low levels of integration and high levels of evolvability characterizes all primates (Figs. 2, 3).

This study finds that *all* primates share a common pattern of integration and evolvability, and differ from each other only in the relative magnitudes of these measures. Whether *Homo* is the most evolvable of the hominoids is not particularly relevant if all primates are characterized by a similarly high degree of evolvability; instead, the patterns of integration and evolvability that are common to all primates may have facilitated adaptation to bipedality during the climatic shifts and accompanying changes in selection pressures of the Pliocene.

References

Ackermann, R. R., & Cheverud, J. M. (2000). Phenotypic covariance structure in tamarins (genus *Saguinus*): A comparison of variation patterns using matrix correlation and common principal component analysis. *American Journal of Physical Anthropology, 111*, 489–501.

Adair, F. (1918). The ossification centers of the fetal pelvis. *The American Journal of Obstetrics and Diseases of Women and Children, 78*, 175–199.

Anemone, R. (1993). The functional anatomy of the hip and thigh in primates. In D. L. Gebo (Ed.), *Postcranial adaptation in nonhuman primates* (pp. 150–174). DeKalb, IL: Northern Illinois University Press.

Arnold, C., Matthews, L. J., & Nunn, C. L. (2010). The 10kTrees website: A new online resource for primate phylogeny. *Evolutionary Anthropology, 19*, 114–118.

Ashton, E. H., Flinn, R. M., Moore, W. J., Oxnard, C. E., & Spence, T. F. (1981). Further quantitative studies of form and function in the primate pelvis with special reference to *Australopithecus*. *The Transactions of the Zoological Society of London, 36*, 1–98.

Atchley, W. R., & Hall, B. K. (1991). A model for development and evolution of complex morphological structures. *Biological Review, 66*, 101–157.

Bastir, M., & Rosas, A. (2009). Mosaic evolution of the basicranium in *Homo* and its relation to modular development. *Evolutionary Biology, 36*, 57–70.

Berger, L. R., de Ruiter, D. J., Churchill, S. E., Schmid, P., Carlson, K. J., Dirks, P. H. G. M., et al. (2010). *Australopithecus sediba*: A new species of *Homo*-like australopith from South Africa. *Science, 328*, 195–204.

Blomberg, S. P., Garland, T., Jr., & Ives, A. R. (2003). Testing for phylogenetic signal in comparative data: Behavioral traits are more labile. *Evolution, 57*(4), 717–745.

Bookstein, F. L. (1991). *Morphometric tools for landmark data: Geometry and biology*. New York: Cambridge University press.

Bramble, D. M., & Lieberman, D. E. (2004). Endurance running and the evolution of *Homo*. *Nature, 432*, 345–352.

Carrier, D. R., Chase, K., & Lark, K. G. (2005). Genetics of canid skeletal variation: Size and shape of the pelvis. *Genome Research, 15*(12), 1825–1830.

Chevallier, A. (1977). Origine des ceintures scapulaires et pelviennes chez l'embryon d'oiseau. *Journal of Embryology and Experimental Morphology, 42*, 275–292.

Cheverud, J. M. (1982). Phenotypic, genetic, and environmental morphological integration in the cranium. *Evolution, 36*(3), 499–516.

Cheverud, J. M. (1988). A comparison of genetic and phenotypic correlations. *Evolution, 42*(5), 958–968.

Cheverud, J. M. (1995). Morphological integration in the saddle-back tamarin (*Saguinus fuscicollis*) cranium. *American Naturalist, 145*(1), 63–89.

Cheverud, J. M. (1996a). Developmental integration and the evolution of pleiotropy. *American Zoologist, 36*, 44–50.

Cheverud, J. M. (1996b). Quantitative genetic analysis of cranial morphology in the cotton-top (*Saguinus oedipus*) and saddle-back (*S. fuscicollis*) tamarins. *Journal of Evolutionary Biology, 9*, 5–42.

Cheverud, J. M., & Marroig, G. (2007). Comparing covariance matrices: Random skewers method compared to the common principal components model. *Genetics and Molecular Biology, 30*(2), 461–469.

Cheverud, J. M., Wagner, G. P., & Dow, M. M. (1989). Methods for the comparative analysis of variation patterns. *Systematic Zoology, 38*(3), 201–213.

Dryden, I. L., & Mardia, K. V. (1998). *Statistical shape analysis*. New York: Wiley.

Escoufier, Y. (1973). Le traitement des variables vectorielles. *Biometrics, 29*, 751–760.

Fleagle, J. G., & Anapol, F. C. (1992). The indriid ischium and the hominid hip. *Journal of Human Evolution, 22*, 285–305.

Goswami, A. (2006a). Cranial modularity shifts during mammalian evolution. *American Naturalist, 168*(2), 270–280.

Goswami, A. (2006b). Morphological integration in the carnivoran skull. *Evolution, 60*(1), 169–183.

Goswami, A., & Polly, P. D. (2010). The influence of modularity on cranial morphological disparity in carnivora and primates (Mammalia). *PLoS ONE, 5*(3), e9517. doi:10.1371/journal.pone.0009517.

Grabowski, M. W., Polk, J. D., & Roseman, C. C. (2011). Divergent patterns of integration and reduced constraint in the human hip and the origins of bipedalism. *Evolution, 65*(5), 1336–1356.

Hallgrímsson, B., Jamniczky, H., Young, N. M., Rolian, C., Parsons, T. E., Boughner, J. C., et al. (2009). Deciphering the palimpsest: Studying the relationship between morphological integration and phenotypic covariation. *Evolutionary Biology, 36*, 355–376.

Hallgrímsson, B., & Lieberman, D. E. (2008). Mouse models and the evolutionary developmental biology of the skull. *Integrative and Comparative Biology, 48*(3), 373–384.

Hallgrímsson, B., Willmore, K., & Hall, B. K. (2002). Canalization, developmental stability, and morphological integration in primate limbs. *Yearbook of Physical Anthropology, 45*, 131–158.

Hansen, T. F., & Houle, D. (2004). Evolvability, stabilizing selection, and the problem of stasis. In M. Pigliucci & K. Preston (Eds.), *Phenotypic integration: Studying the ecology and evolution of complex phenotypes* (pp. 130–153). Cary, NC: Oxford University Press.

Hansen, T. F., & Houle, D. (2008). Measuring and comparing evolvability and constraint in multivariate characters. *Journal of Evolutionary Biology, 21*, 1201–1219.

Harmon, L. J., & Glor, R. E. (2010). Poor statistical performance of the mantel test in phylogenetic comparative analyses. *Evolution, 64*(7), 2173–2178.

Harmon, L. J., Weir, J. T., Brock, C. D., Glor, R. E., & Challenger, W. (2008). GEIGER: Investigating evolutionary radiations. *Bioinformatics, 24*, 129–131.

Jouffroy, F. K. (1975). Osteology and myology of the lemuriform postcranial skeleton. In I. Tattersall & R. W. Sussman (Eds.), *Lemur biology* (pp. 149–192). New York: Plenum Press.

Jungers, W. L. (1976). Hindlimb and pelvic adaptations to vertical climbing and clinging in *Megaladapis*, a giant subfossil prosimian from Madagascar. *Yearbook of Physical Anthropology, 20*, 508–524.

Kembel, S. W., Cowan, P. D., Helmus, M. R., Cornwell, W. K., Morlon, H., Ackerly, D. D., et al. (2010). Picante: R tools for integrating phylogenies and ecology. *Bioinformatics, 26*, 1463–1464.

Klingenberg, C. P. (2008). Morphological integration and developmental modularity. *Annual Review of Ecology, Evolution, and Systematics, 39*, 115–132.

Klingenberg, C. P. (2009). Morphometric integration and modularity in configurations of landmarks: Tools for evaluating a priori hypotheses. *Evolution & Development, 11*(4), 405–421.

Klingenberg, C. P. (2011). MorphoJ: An integrated software package for geometric morphometrics. *Molecular Ecology Resources, 11*, 353–357.

Lande, R. (1979). Quantitative genetic analysis of multivariate evolution, applied to brain: Body size allometry. *Evolution, 33*, 402–416.

Laurenson, R. D. (1964). The chondrification of the human ilium. *The Anatomical Record, 148*, 197–202.

Lewton, K. L. (2010). *Locomotor function and the evolution of the primate pelvis [Ph.D.]*. Tempe: Arizona State University.

Lleonart, J., Salat, J., & Torres, G. J. (2000). Removing allometric effects of body size in morphological analysis. *Journal of Theoretical Biology, 205*, 85–93.

Lovejoy, C. O. (1975). Biomechanical perspectives on the lower limb of early hominids. In R. H. Tuttle (Ed.), *Primate functional morphology and evolution* (pp. 291–326). Chicago: Aldine.

Lovejoy, C. O., Suwa, G., Spurlock, L., Asfaw, B., & White, T. D. (2009). The pelvis and femur of *Ardipithecus ramidus*: The emergence of upright walking. *Science, 326*(5949), 71–77.

MacLatchy, L. (1998). Reconstruction of hip joint function in extant and extinct fossil primates. In E. Strasser, J. G. Fleagle, A. Rosenberger, & H. M. McHenry (Eds.), *Primate locomotion: Recent advances* (pp. 111–130). New York: Plenum Press.

Malashichev, Y., Borkhvardt, V., Christ, B., & Scaal, M. (2005). Differential regulation of avian pelvic girdle development by the limb field ectoderm. *Anatomy and Embryology, 210*, 187–197.

Malashichev, Y., Christ, B., & Prols, F. (2008). Avian pelvis originates from lateral plate mesoderm and its development requires signals from both ectoderm and paraxial mesoderm. *Cell and Tissue Research, 331*, 595–604.

Manly, B. F. J. (1997). *Randomization, bootstrap and Monte Carlo methods in biology*. Boca Raton, FL: CRC Press.

Marroig, G., & Cheverud, J. M. (2001). A comparison of phenotypuc variation and covariation patterns and the role of phylogeny, ecology, and ontogeny during cranial evolution of new world monkeys. *Evolution, 55*, 2576–2600.

Marroig, G., & Cheverud, J. M. (2004a). Cranial evolution in sakis (*Pithecia*, Platyrrhini) I: Interspecific differentiation and allometric patterns. *American Journal of Physical Anthropology, 125*, 266–278.

Marroig, G., & Cheverud, J. M. (2004b). Did natural selection or genetic drift produce the cranial diversification of neotropical monkeys? *American Naturalist, 163*(3), 417–428.

Marroig, G., Shirai, L. T., Porto, A., de Oliveira, F. B., & De Conto, V. (2009). The evolution of modularity in the mammalian skull II: Evolutionary consequences. *Evolutionary Biology, 36*, 136–148.

McNulty, K. P. (2005). A geometric morphometric assessment of the hominoid supraorbital region: Affinities of the Eurasian Miocene hominoids *Dryopithecus*, *Graecopithecus*, and *Sivapithecus*. In D. E. Slice (Ed.), *Modern morphometrics in physical anthropology* (pp. 349–373). New York: Kluwer.

Mitteroecker, P., & Bookstein, F. (2008). The evolutionary role of modularity and integration in the hominoid cranium. *Evolution, 62*(4), 943–958.

Olson, E. C., & Miller, R. L. (1958). *Morphological integration*. Chicago: University of Chicago Press.

O'Rahilly, R., & Gardner, E. (1975). The timing and sequence of events in the development of the limbs in the human embryo. *Anatomy and Embryology, 148*, 1–23.

Pavlicev, M., Cheverud, J. M., & Wagner, G. P. (2009). Measuring morphological integration using eigenvalue variance. *Evolutionary Biology, 36*, 157–170.

Pellegrini, M., Pantano, S., Fumi, M. P., Lucchini, F., & Forabosco, A. (2001). Agenesis of the scapula in *Emx2* homozygous mutants. *Developmental Biology, 232*, 149–156.

Pomikal, C., Blumer, R., & Streicher, J. (2011). Four-dimensional analysis of early pelvic girdle development in *Rana temporaria*. *Journal of Morphology, 272*, 287–301.

Pomikal, C., & Streicher, J. (2010). 4D-analysis of early pelvic girdle development in the mouse (*Mus musculus*). *Journal of Morphology, 271*(1), 116–126.

Porto, A., de Oliveira, F. B., Shirai, L. T., de Conto, V., & Marroig, G. (2009). The evolution of modularity in the mammalian skull I: Morphological integration patterns and magnitudes. *Evolutionary Biology, 36*, 118–135.

R Development Core Team. (2011). *R: A language and environment for statistical computing*. Vienna: R Foundation for Statistical Computing.

Revell, L. (2007). Skewers: A program for Cheverud's random skewers method of matrix comparison. http://anolis.oeb.harvard.edu/∼liam/programs/.

Riedl, R. (1977). A systems-analytical approach to macro-evolutionary phenomena. *The Quarterly Review of Biology, 52*, 351–370.

Robinson, J. T. (1972). *Early hominid posture and locomotion*. Chicago: The University of Chicago Press.

Rohlf, F. J., & Slice, D. (1990). Extensions of the Procrustes method for the optimal superimposition of landmarks. *Systematic Zoology, 39*(1), 40–59.

Rolian, C. (2009). Integration and evolvability in primate hands and feet. *Evolutionary Biology, 36*(1), 100–117.

Scott, J. E. (2010). *Nonsocial influences on canine size in anthropoid primates [Ph.D.]*. Tempe: Arizona State University.

Sigmon, B. A., & Farslow, D. L. (1986). The primate hindlimb. In D. R. Swindler & J. Erwin (Eds.), *Comparative primate biology, volume 1: Systematics, evolution, and anatomy* (pp. 671–718). New York: Alan R. Liss, Inc.

Steppan, S. J. (2004). Phylogenetic comparisons of multivariate data. In M. Piglicucci & K. Preston (Eds.), *Phenotypic integration: Studying the ecology and evolution of complex phenotypes* (pp. 325–344). New York: Oxford University Press.

Stern, J. T., & Susman, R. L. (1983). The locomotor anatomy of *Australopithecus afarensis*. *American Journal of Physical Anthropology, 60*, 279–312.

Strait, D. S. (2001). Integration, phylogeny, and the hominid cranial base. *American Journal of Physical Anthropology, 114*, 273–297.

Tague, R. G. (2005). Big-bodied males help us recognize that females have big pelves. *American Journal of Physical Anthropology, 127*, 392–405.

Villmoare, B., Fish, J., & Jungers, W. (2011). Selection, morphological integration, and strepsirrhine locomotor adaptations. *Evolutionary Biology, 38*(1), 88–99.

Wagner, G. P. (1984). On the eigenvalue distribution of genetic and phenotypic dispersion matrices: Evidence for a nonrandom organization of quantitative character variation. *Journal of Mathematical Biology, 21*, 77–95.

Wagner, G. P. (1996). Homologues, natural kinds and the evolution of modularity. *American Zoologist, 36*(1), 36–43.

Williams, S. A. (2010). Morphological integration and the evolution of knuckle-walking. *Journal of Human Evolution, 58*, 432–440.

Willis, J. H., Coyne, J. A., & Kirkpatrick, M. (1991). Can one predict the evolution of quantitative characters without genetics? *Evolution, 45*, 441–444.

Young, N. M. (2006). Function, ontogeny and canalization of shape variance in the primate scapula. *Journal of Anatomy, 209*, 623–636.

Young, N. M., & Hallgrímsson, B. (2005). Serial homology and the evolution of mammalian limb covariation structure. *Evolution, 59*, 2691–2704.

Young, N. M., Wagner, G. P., & Hallgrímsson, B. (2010). Development and the evolvability of human limbs. *Proceedings of the National Academy of Science, 107*, 3400–3405.

Zelditch, M. L., Wood, A. R., & Swiderski, D. L. (2009). Building developmental integration into functional systems: Function-induced integration of mandibular shape. *Evolutionary Biology, 36*, 71–87.